

# Top3DFVT: Topology optimization algorithm for three-dimensional continuum elastic structures applying the finite-volume theory

Arnaldo dos Santos Júnior<sup>1</sup>, Marcelo Vitor Oliveira Araujo<sup>1</sup>, Romildo dos Santos Escarpini Filho<sup>2</sup>, Eduardo Nobre Lages<sup>1</sup>, Márcio André Araújo Cavalcante<sup>3</sup>

<sup>1</sup>*Center of Technology, Federal University of Alagoas*

*Av. Lourival Melo Mota, Tabuleiro do Martins, 57072-900, Maceió/AL, Brazil  
arnaldojunioral@gmail.com, marcelo.vitor.o.a@gmail.com, enl@lccv.ufal.br*

<sup>2</sup>*Campus Arapiraca, Federal University of Alagoas*

*Avenida Divaldo Suruagy, 57200-000, Penedo/AL, Brazil  
romildo.escarpini@penedo.ufal.br*

<sup>3</sup>*Campus of Engineering and Agricultural Sciences, Federal University of Alagoas*

*BR 104, Km 85, 57100-000, Rio Largo/AL, Brazil  
marcio.cavalcante@ceca.ufal.br*

**Abstract.** Topology optimization is a powerful computational tool for determining optimal material layouts within a design domain, aiming to minimize structural compliance under a prescribed volume constraint. Conventional density-based approaches, such as the solid isotropic material with penalization (SIMP) and the rational approximation of material properties (RAMP), are widely employed to interpolate material properties and drive the solution toward discrete “black-and-white” topologies. Although most topology optimization frameworks rely on the finite element method (FEM), alternative discretization strategies, such as the finite-volume theory (FVT), have demonstrated promising capabilities, particularly in addressing numerical issues like checkerboard patterns in the absence of filtering techniques. The proposed formulation employs compatibility and continuity conditions in the surface-averaged sense at the subvolume faces and locally satisfies the equilibrium equations at the subvolume level, providing a physically consistent basis for structural analysis. This work presents an extension of a density-based topology optimization algorithm grounded in the standard finite-volume theory for three-dimensional linear elastic structures. The numerical formulation adopts structured meshes and an artificial interpolation scheme to enhance solution discreteness and stability. In addition, an adaptation of the optimality criteria (OC) method is adopted, aimed at suppressing gray scales, employing a linear relationship between material stiffness and density (Voigt model of micromechanics) instead of a penalization of intermediate densities approach. The formulation’s effectiveness is demonstrated through numerical examples, establishing it as a promising alternative for 3D topology optimization.

**Keywords:** 3D topology optimization, Continuum elastic structures, Finite-volume theory, MATLAB code.

## 1 Introduction

Topology optimization is a well-established computational methodology used by engineers to determine optimal material layouts within a predefined design domain. In structural mechanics, a commonly addressed objective is the minimization of structural compliance under a volume constraint, aiming for a material distribution where the relative density approaches either 1 (solid) or 0 (void), under prescribed loading conditions. However, due to the discrete nature of material assignment, the problem is inherently non-convex and difficult to solve directly. To overcome this challenge, researchers typically reformulate it as a continuous optimization problem by interpolating material properties (Bendsøe and Sigmund [1]). In this context, two of the most widely used interpolation schemes are the solid isotropic material with penalization (SIMP) model, initially proposed by Bendsøe [2] and further popularized by Rozvany et al. [3], and the rational approximation of material properties

(RAMP) model, introduced by Stolpe and Svanberg [4]. These techniques specifically penalize intermediate density values, thus favoring the emergence of clear “black-and-white” topologies. Both schemes have been extensively incorporated into gradient-based optimization algorithms and integrated within finite-element solvers.

Several benchmark implementations with the finite element method (FEM) have helped researchers disseminate and verify topology optimization techniques. Notable examples include the classical **top99** code introduced by Sigmund [5] and the **top88** by Andreassen et al. [6], frequently recommended as a starting point due to their clarity and educational value for topology optimization of two-dimensional structures. A compact 3D extension of the well-known **top88** code, developed by Liu and Tovar [7] and commonly referred to as **top3d**, offers a clear and self-contained platform for finite-element analysis and has become a widely adopted tool in academia for teaching three-dimensional topology optimization, and is frequently recommended for students and researchers entering the field of structural topology optimization.

Building upon the educational foundation of compact topology optimization codes, Ferrari and Sigmund [8] introduced **top99neo**, an efficient extension of the original 99-line MATLAB code. This algorithm streamlines matrix assembly and incorporates vectorized operations for improved performance, which they also extended to three-dimensional problems through the **top3D125** version. Among the notable advancements inspired by such frameworks is **PolyTop3D** (Chi et al. [9]), a high-performance and extensible MATLAB implementation tailored for large-scale 3D structural optimization, and **FreeTop** (Ibhadode et al. [10]), a novel open-source MATLAB code to address common limitations in topology optimization frameworks, such as restricted domain initialization and the absence of CAD-compatible output, by allowing the definition of arbitrary 3D geometries and generating Standard Triangle Language (STL) files after optimization. Most of these codes employ the finite element method for domain discretization and structural response evaluation, establishing a standard foundation for research and teaching in topology optimization. Complementing these developments, Yago et al. [11] provide an exhaustive comparative study of representative 3D topology optimization methods, including SIMP, Level-set, BESO, and VARTOP, evaluating their computational cost, topology quality, objective function performance, and robustness through industrial-scale benchmark problems.

Despite the robustness of FEM, several numerical artifacts, such as checkerboard patterns and mesh dependency, persist in topology optimization, particularly in the absence of filtering or regularization techniques. In this sense, researchers have explored alternative discretization schemes in response to these challenges. Among them, the finite-volume theory (FVT) has emerged as an alternative, derived initially from higher-order theories for functionally graded materials (Aboudi et al. [12]). Unlike conventional finite element methods, FVT is independently formulated and characterized by the enforcement of local and global equilibrium equations using surface-averaged quantities and interfacial continuity conditions (Bansal and Pindera [13]; Zhong et al. [14]). The application of the finite-volume theory to density-based topology optimization has shown promising results in two-dimensional problems, particularly in suppressing checkerboard patterns without the need for additional filtering techniques, as demonstrated by Araujo et al. [15, 16, 17]. Among these, [17] details **Top2DFVT**, an efficient MATLAB implementation inspired by the well-known **top88** and **top99neo** codes. It achieves high computational performance by leveraging sparse matrix operations, streamlined assembly procedures, and a compact data structure, enabling fast convergence with reduced computational cost.

The present work advances this line of research by extending the FVT-based topology optimization approach to three-dimensional linear elastic structures through the development of the **TOP3DFVT** code. The proposed formulation adopts structured meshes and incorporates both SIMP and RAMP interpolation models in the numerical implementation. Furthermore, to mitigate the appearance of intermediate gray regions, a modified optimality criteria (OC) algorithm, based on the heuristic proposed by Groenwold and Etman [18], is employed to enhance numerical convergence and promote the emergence of discrete, “black-and-white” design configurations.

## 2 Theoretical background

### 2.1 The standard finite-volume theory

The proposed formulation builds upon the work of Cavalcante and Pindera [19, 20] within the standard, or zeroth-order, finite-volume theory framework for rectangular discretization. In this formulation, static variables are represented as surface-averaged tractions, while kinematic variables are defined as surface-averaged

displacements along the edges. Extending this to three dimensions involves discretizing a regular prismatic domain into  $N_q$  subvolumes. Figure 1 illustrates this discretization, defining global coordinates  $x_i$  (for  $i = 1, 2, 3$ ), local coordinates  $x_i^{(q)}$ , and subvolume dimensions  $l_q$ ,  $h_q$  and  $b_q$ . The displacement field components in 3D are represented by an incomplete quadratic approximation using a second-order Legendre polynomial in the local coordinate system as follows:

$$u_i^{(q)} = W_{i(000)}^{(q)} + x_1^{(q)} W_{i(100)}^{(q)} + x_2^{(q)} W_{i(010)}^{(q)} + x_3^{(q)} W_{i(001)}^{(q)} + \frac{1}{2} \left( 3(x_1^{(q)})^2 - \frac{l_q^2}{4} \right) W_{i(200)}^{(q)} + \frac{1}{2} \left( 3(x_2^{(q)})^2 - \frac{h_q^2}{4} \right) W_{i(020)}^{(q)} + \frac{1}{2} \left( 3(x_3^{(q)})^2 - \frac{b_q^2}{4} \right) W_{i(002)}^{(q)}, \quad (1)$$

where  $W_{i(mno)}^{(q)}$  represent the unknown coefficients of the displacement field.

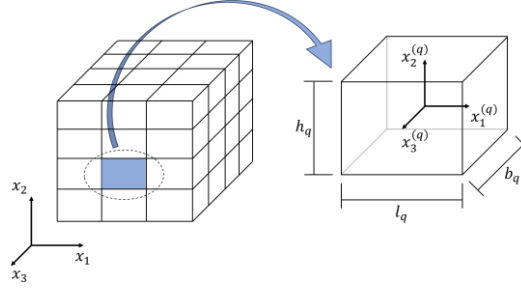


Figure 1. Discretized analysis domain and global coordinate system (left) and subvolume or local coordinate system (right)

The standard finite-volume theory defines kinematic and static variables as surface-averaged displacements and tractions on the subvolume faces, respectively (see Figure 2). The faces are indexed as: 1 (left), 2 (right), 3 (bottom), 4 (top), 5 (back), and 6 (front). Surface-averaged displacements on each face are computed via integrals using the displacement field approximation from Eq. (1) as follows:

$$\begin{aligned} \bar{u}_i^{(q,f=1,2)} &= \frac{1}{h_q b_q} \int_{-b_q/2}^{b_q/2} \int_{-h_q/2}^{h_q/2} u_i^{(q)}(\mp l_q/2, x_2^{(q)}, x_3^{(q)}) dx_2^{(q)} dx_3^{(q)} = W_{i(000)}^{(q)} \mp \frac{l_q}{2} W_{i(100)}^{(q)} + \frac{l_q^2}{4} W_{i(200)}^{(q)}, \\ \bar{u}_i^{(q,f=3,4)} &= \frac{1}{l_q b_q} \int_{-b_q/2}^{b_q/2} \int_{-l_q/2}^{l_q/2} u_i^{(q)}(x_1^{(q)}, \mp h_q/2, x_3^{(q)}) dx_1^{(q)} dx_3^{(q)} = W_{i(000)}^{(q)} \mp \frac{h_q}{2} W_{i(010)}^{(q)} + \frac{h_q^2}{4} W_{i(020)}^{(q)}, \\ \bar{u}_i^{(q,f=5,6)} &= \frac{1}{l_q h_q} \int_{-h_q/2}^{h_q/2} \int_{-l_q/2}^{l_q/2} u_i^{(q)}(x_1^{(q)}, x_2^{(q)}, \mp b_q/2) dx_1^{(q)} dx_2^{(q)} = W_{i(000)}^{(q)} \mp \frac{b_q}{2} W_{i(001)}^{(q)} + \frac{b_q^2}{4} W_{i(002)}^{(q)}, \end{aligned} \quad (2)$$

where  $\bar{u}_i^{(q,f)}$  are the surface-averaged displacement for the indexed face  $f$  of a generic subvolume  $q$ .

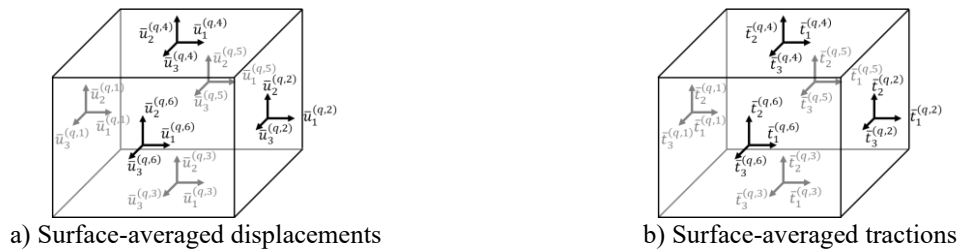


Figure 2. Surface-averaged kinematic and static variables for a generic subvolume  $q$

The eighteen expressions presented in Eq. (2) can be rearranged in terms of the surface-averaged displacements as a function of the unknown coefficients as:

$$\bar{\mathbf{u}}^{(q)} = \mathbf{A}_{(18 \times 18)}^{(q)} \mathbf{W}^{(q)} + \mathbf{a}_{(18 \times 3)}^{(q)} \mathbf{W}_{(0)}^{(q)}, \quad (3)$$

where  $\bar{\mathbf{u}}^{(q)}$  is the local surface-averaged displacement vector,  $\mathbf{W}^{(q)}$  is the vector containing the first and second

order unknown coefficients,  $\mathbf{W}_{(0)}^{(q)}$  is the vector containing the zeroth order unknown coefficients, and  $\mathbf{A}_{(18 \times 18)}^{(q)}$  and  $\mathbf{a}_{(18 \times 3)}^{(q)}$  are matrices depending on the geometric features of the subvolumes.

Similarly to the kinematic case, the standard finite-volume theory evaluates static variables as surface-averaged tractions acting on the subvolume faces (Figure 2). Considering the stress tensor for a linear elastic isotropic material, the surface-averaged tractions can be obtained employing Cauchy's relation. These surface tractions represent the static variables in the finite-volume framework and are essential for enforcing the local-equilibrium conditions across the subvolumes, which gives:

$$\bar{\mathbf{t}}^{(q)} = \mathbf{B}_{(18 \times 18)}^{(q)} \mathbf{W}^{(q)}, \quad (4)$$

where  $\mathbf{B}_{(18 \times 18)}^{(q)}$  is composed of elements that depend on the subvolume dimensions and material properties. Imposing the local equilibrium condition from Eq. (4) on a subvolume without body forces by summing the surface-averaged tractions over its six faces ( $\sum_{f=1}^6 \bar{\mathbf{t}}^{(q,f)} S_f^{(q)} = \mathbf{0}_{(3 \times 1)}$ ), weighted by their faces areas  $S_f^{(q)}$ , results in the following local system of equations for a generic subvolume:

$$\bar{\mathbf{t}}^{(q)} = \mathbf{K}_{(18 \times 18)}^{(q)} \bar{\mathbf{u}}^{(q)}, \quad (5)$$

where  $\mathbf{K}_{(18 \times 18)}^{(q)} = \mathbf{B}_{(18 \times 18)}^{(q)} \bar{\mathbf{A}}_{(18 \times 18)}^{(q)}$  is the local stiffness matrix. However, it is unusual to have a system of equations that relates tractions and displacements. Additionally, the matrix  $\mathbf{K}_{(18 \times 18)}^{(q)}$  is not symmetric, which requires an additional computational cost to solve this kind of problem. The proposed formulation overcomes this limitation by introducing energetically conjugate quantities (forces and displacements), which consequently allows the evaluation of the resultant forces on the subvolume faces as follows:

$$R_i^{(q,f)} = \int_{S^{(q)}} t_i^{(q,f)}(x_1^{(q)}, x_2^{(q)}, x_3^{(q)}) dS^{(q)} = S_f^{(q)} \bar{t}_i^{(q,f)}. \quad (6)$$

Then, the local system of equations (Eq. 5) can be modified and rewritten as

$$\mathbf{R}^{(q)} = \mathbf{S}_{(18 \times 18)}^{(q)} \bar{\mathbf{t}}^{(q)} = \mathbf{S}_{(18 \times 18)}^{(q)} \mathbf{K}_{(18 \times 18)}^{(q)} \bar{\mathbf{u}}^{(q)} = \bar{\mathbf{K}}_{(18 \times 18)}^{(q)} \bar{\mathbf{u}}^{(q)}, \quad (7)$$

where  $\mathbf{R}^{(q)}$  is the local resultant force vector,  $\bar{\mathbf{K}}_{(18 \times 18)}^{(q)} = \mathbf{S}_{(18 \times 18)}^{(q)} \mathbf{K}_{(18 \times 18)}^{(q)}$  is the modified local stiffness matrix, which is a symmetric matrix that relates the local resultant force and displacement vectors, and  $\mathbf{S}^{(q)}$  is a matrix with the subvolume faces areas. Finally, the global stiffness matrix is assembled by summing the contributions of all subvolumes, resulting in the following global system of equations:

$$\mathbf{R}_{(ndof \times 1)} = \bar{\mathbf{K}}_{(ndof \times ndof)} \mathbf{U}_{(ndof \times 1)}, \quad (8)$$

where  $\mathbf{R}_{(ndof \times 1)}$  and  $\mathbf{U}_{(ndof \times 1)}$  are the global force and displacement vectors,  $\bar{\mathbf{K}}_{(ndof \times ndof)}$  is the global stiffness matrix, and  $ndof$  is the total number of degrees of freedom.

## 2.2 Topology optimization

The study integrates density-based topology optimization (SIMP and RAMP) with finite-volume theory to minimize the compliance of three-dimensional linear elastic structures by introducing an artificial density field and employing a nonlinear interpolation scheme to define material properties. This approach effectively guides the design toward distinct solid and void regions, as expressed in the general formulation presented in Eq. (9).

$$\begin{aligned} & \text{find } \boldsymbol{\rho} = \{\rho_1, \rho_2, \dots, \rho_{N_q}\}^T, \text{ that} \\ & \text{minimize}_{\boldsymbol{\rho}} c(\boldsymbol{\rho}) = \sum_{q=1}^{N_q} \mathbf{R}^{(q)T} \bar{\mathbf{u}}^{(q)}, \\ & \text{subject to: } \bar{\mathbf{K}}_{(ndof \times ndof)} \mathbf{U}_{(ndof \times 1)} = \mathbf{R}_{(ndof \times 1)}, \\ & \quad \frac{1}{\Omega} \sum_{q=1}^{N_q} v_q \rho_q \leq \vartheta, \\ & \quad 0 \leq \rho_q \leq 1, q = 1, \dots, N_q, \end{aligned} \quad (9)$$

where  $\rho$  corresponds to the relative density vector,  $c(\rho)$  is the objective function (compliance),  $v_q$  denotes the volume of the  $q$ th subvolume,  $\vartheta$  corresponds to a prescribed volume fraction constraint, and  $N_q$  is the number of subvolumes. However, conventional material penalization methods often lead to optimized topologies that retain intermediate-density gray regions. To address this issue, the gray scale suppression (GSS) strategy (Groenwold and Etman [17]) penalizes intermediate densities, effectively guiding the optimization toward crisp, manufacturable topologies. This strategy employs a power-law gray scale suppression, resulting in the modified OC formulation for the new density variable ( $\rho_q^{new}$ ) as follows:

$$\rho_q^{new} = \max \left\{ 0, \max \left\{ \rho_q - m, \min \left\{ 1, \min \left\{ \rho_q + m, [\rho_q (\beta_q)^\eta]^r \right\} \right\} \right\} \right\}, \quad (10)$$

where  $m$  is a positive move limit,  $\eta$  is a numerical damping factor,  $r \geq 1$  is GSS parameter, and  $\beta_q$  is the optimality condition evaluated by:

$$\beta_q = -\frac{\partial c}{\partial \rho_q} \left( \lambda \frac{\partial v}{\partial \rho_q} \right)^{-1}, \quad (11)$$

with  $\lambda$  representing the positive Lagrangian multiplier, which can be determined using a bisection algorithm to enforce the satisfaction of the constraint on the volume fraction ( $\vartheta$ ).

### 3 Matlab implementation

The proposed methodology is implemented in the **TOP3DFVT** MATLAB code, designed as a compact and educational tool for three-dimensional structural topology optimization employing the standard finite-volume theory. Designed to support structured meshes and integrate both SIMP and RAMP interpolation models, allowing flexibility in material penalization strategies. Additionally, a gray scale suppression scheme is available, employing a linear interpolation (Voigt model) to promote crisp “black-and-white” topologies. The optimization routine follows a modified optimality criteria algorithm, which iteratively updates the material density field based on compliance sensitivity analysis and a volume constraint. The code structure prioritizes vectorized operations and sparse matrix assembly to ensure computational efficiency, while real-time 3D visualizations assist in monitoring the evolution of the topology. The **TOP3DFVT** source code is openly available at: <https://github.com/arnaldojunior/TOP3DFVT>.

### 4 Numerical results

To assess the stability of the new 3D finite-volume approach for topology optimization of structures, the classical Cantilever beam problem is analyzed, focusing on compliance minimization. The boundary conditions and mesh discretization employed are illustrated in Figure 3. For simplicity, the geometry of the beam is defined by the number of subvolumes used for the mesh discretization (30 x 10 x 3). The material properties are  $E = 1$  (Young’s modulus), a minimum modulus value of  $E_{min} = 10^{-9}$  to prevent singularity in the global stiffness matrix,  $\nu = 0.3$  (Poisson ratio). The load is distributed uniformly along the beam’s right border by applying the same force to each subvolume face, so that the resultant force equals 1.

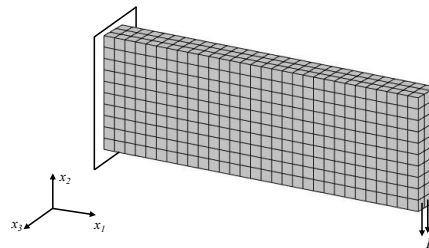


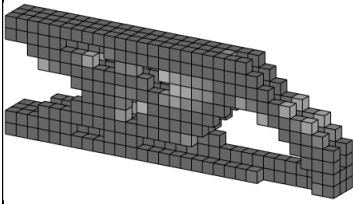
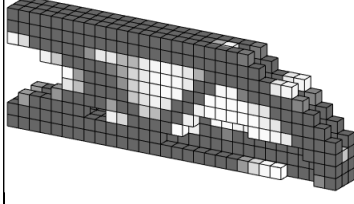
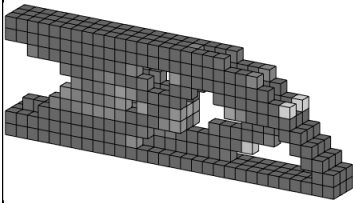
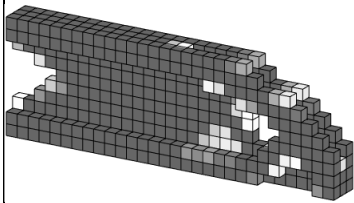
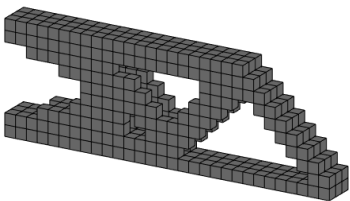
Figure 3. 3D cantilever beam boundary conditions and mesh discretization

The numerical analyses are conducted **without filtering techniques**, using the optimization parameter

dumping factor  $\eta = 1/3$ , strategically selected to regularize displacement oscillations in less dense regions during the iterative process and to avoid the oscillatory phenomena that can occur in analyses without a filtering scheme with the FVT simulations, particularly for the SIMP method, as observed by Araujo et al. [14, 15, 16]. The move limit is set to  $m = 0.2$ , and the optimization is considered converged when the maximum change in design variables between successive iterations falls below the user-defined tolerance of  $tol = 0.001$ , considering a fixed solid material volume fraction constraint of 50%. The GSS parameter varies gradually from 1 to 3, with increments of 1.02 times  $r$  starting from iteration 20 onwards.

Table 1 presents a comparative analysis of different material penalization strategies integrated with the GSS strategy. The results are evaluated in terms of structural compliance ( $c$ ) and the percentage of “black-and-white” elements (B&W), which reflect the discreteness of the optimized topology. Under fixed penalization, the SIMP method ( $p = 4$ ) yields a relatively high discreteness (88.56%) but with elevated compliance ( $c = 668.93$ ). In contrast, RAMP ( $p = 3$ ) achieves lower compliance ( $c = 612.29$ ), albeit at the cost of a reduced “black-and-white” percentage (73.11%), indicating a higher presence of intermediate densities. The continuation scheme, where the penalization factor is gradually increased, improves both performance metrics. RAMP ( $p = 0:3$ ) demonstrates the best trade-off, achieving the lowest compliance ( $c = 582.84$ ) and a significantly high “black-and-white” percentage (90.89%). SIMP also benefits from continuation, reaching  $c = 622.76$  and B&W = 88.33%. Finally, the GSS strategy alone results in a fully discrete topology (B&W = 100%) with compliance  $c = 636.21$ , outperforming fixed penalization methods in topology clarity. Although its compliance is slightly higher than the best continuation-based RAMP result, GSS proves highly effective in eliminating gray regions without requiring continuation schemes. These results confirm that the GSS strategy is a robust alternative for promoting manufacturable topologies while maintaining acceptable structural performance.

Table 1. Comparison of topology optimization methods with the gray scale suppression strategy

Fixed penalization	
SIMP ( $p = 4$ )	RAMP ( $p = 3$ )
 <p><math>c = 668.93</math> B&amp;W = 88.56%</p>	 <p><math>c = 612.29</math> B&amp;W = 73.11%</p>
Continuation scheme	
SIMP ( $p = 1:4$ )	RAMP ( $p = 0:3$ )
 <p><math>c = 622.76</math> B&amp;W = 88.33%</p>	 <p><math>c = 582.84</math> B&amp;W = 90.89%</p>
Gray scale suppression	
 <p><math>c = 636.21</math> B&amp;W = 100%</p>	

## 5 Conclusions

This work introduced a novel three-dimensional topology optimization framework based on the standard

finite-volume theory (FVT), implemented in the educational and compact MATLAB code **TOP3DFVT**. The proposed formulation effectively integrates SIMP and RAMP interpolation models with a modified Optimality Criteria algorithm to promote discrete “black-and-white” topologies. Numerical results demonstrate the stability of the method and its ability to suppress gray scales without relying on additional filtering techniques. These results highlight the potential of the FVT-based approach as a promising alternative to traditional finite-element formulations in structural topology optimization. These preliminary results are encouraging but require more investigation.

**Acknowledgements.** The authors acknowledge the financial support provided by the National Council for Scientific and Technological Development (CNPq), Coordination for the Improvement of Higher Education Personnel (CAPES), and Alagoas State Research Support Foundation (FAPEAL).

**Authorship statement.** The text should be exactly as follows: The authors hereby confirm that they are the sole liable persons responsible for the authorship of this work, and that all material that has been herein included as part of the present paper is either the property (and authorship) of the authors or has the permission of the owners to be included here.

## References

- [1] M. P. Bendsøe, O. Sigmund. *Topology Optimization: Theory, Methods and Applications*. Berlin: Springer, ISBN 978-3-540-42992-1, 2003.
- [2] M. P. Bendsøe. Optimal shape design as a material distribution problem. *Structural Optimization*, v.1, pp. 193–202, 1989.
- [3] G. Rozvany, M. Zhou, T. Birker. Generalized shape optimization without homogenization. *Structural optimization* v. 4, pp. 250–252, 1992.
- [4] M. Stolpe, K. Svanberg. An alternative interpolation scheme for minimum compliance topology optimization. *Structural and Multidisciplinary Optimization*, v. 22, pp. 116–124, 2001.
- [5] O. Sigmund. 99 line topology optimization code written in MATLAB. *Structural and Multidisciplinary Optimization*, v. 21, pp. 120–127, 2001.
- [6] E. Andreassen, A. Clausen, M. Schevenels, J. Laugesen, O. Sigmund. Efficient topology optimization in MATLAB using 88 lines of code. *Structural and Multidisciplinary Optimization*, v. 43, pp. 1–16, 2011.
- [7] K. Liu and A. Tovar. An efficient 3D topology optimization code written in MATLAB. *Structural and Multidisciplinary Optimization*, v. 50, pp. 1175–1196, 2014.
- [8] F. Ferrari and O. Sigmund. Top99neo: An updated 99 line topology optimization code. *Structural and Multidisciplinary Optimization*, v. 62, pp. 2211–2228, 2020.
- [9] H. Chi, K. Liu, S. Shin. PolyTop3D: A compact MATLAB implementation for 3D topology optimization. *Structural and Multidisciplinary Optimization*, v. 62, pp. 1539–1558, 2020.
- [10] O. Ibhádode, Y.F Fu, A. Qureshi. FreeTO – Freeform 3D topology optimization using a structured mesh with smooth boundaries in MATLAB. *Advances in Engineering Software*, v. 198, p. 103790, 2024.
- [11] D. Yago, J. Cante, O. Lloberas-Valls, J. Oliver. Topology Optimization Methods for 3D Structural Problems: A Comparative Study. *Archives of Computational Methods in Engineering*, vol. 29, pp. 1525–1567, 2022.
- [12] J. Aboudi, M.-J. Pindera, S.M. Arnold. Higher-order theory for functionally graded materials. *Composites: Part B*, vol. 30, n. 8, pp. 777-832, 1999.
- [13] Y. Bansal, M.-J. Pindera. Efficient reformulation of the thermoelastic higher-order theory for functionally graded materials. *Journal of Thermal Stress*, vol. 26, n. 11-12, pp. 1055-1092, 2003.
- [14] Y. Zhong, Y. Bansal, M.-J. Pindera. Efficient reformulation of the thermal higher-order theory for FGMs with locally variable conductivity. *International Journal of Computational Science and Engineering*, vol. 5, n. 4, pp. 795-831, 2004.
- [15] M. V. O. Araujo, E. N. Lages, M. A. A. Cavalcante. Checkerboard free topology optimization for compliance minimization applying the finite-volume theory. *Mechanics Research Communications*, vol. 108, n. 103581, 2020a.
- [16] M. V. O. Araujo, E. N. Lages, M. A. A. Cavalcante. Checkerboard-free topology optimization for compliance minimization of continuum elastic structures based on the generalized finite-volume theory. *Latin American Journal of Solids and Structures*, vol. 17, n. 8, pp. 1-21, 2020b.
- [17] M. V. O. Araujo, A. Santos Júnior, R. Escarpini Filho, E. N. Lages, M. A. A. Cavalcante, TOP2DFVT: An Efficient Matlab Implementation for Topology Optimization based on the Finite-Volume Theory. *F1000Research*, vol. 13, n. 805, 2024.
- [18] A. A. Groenwold, L. F. P. Etman, L. F. P. A simple heuristic for gray-scale suppression in topology optimization. *Structural and Multidisciplinary Optimization*, 39, 217–225, 2009.
- [19] M. A. A. Cavalcante, M.-J. Pindera. Generalized finite-volume theory for elastic analysis in solid mechanics – part I: framework. *Journal of Applied Mechanics*, vol.79, n. 5, pp. 051006, 2012.
- [20] M. A. A. Cavalcante, M.-J. Pindera. Generalized finite-volume theory for elastic analysis in solid mechanics – part II: results. *Journal of Applied Mechanics*, vol.79, n. 5, pp. 051007, 2012.